U. S. DEPARTMENT OF THE INTERIOR

U. S. GEOLOGICAL SURVEY

Space-time patterns of Late Cenozoic extension, vertical-axis rotation, and volcanism in the Crater Flat basin, southwest Nevada

by: **C. J. Fridrich[1], J. W. Whitney[1], M. R. Hudson[1], and B. M. Crowe[2]**

1 U. S. Geological Survey, Box 25046, Denver, CO 80225

2 Los Alamos National Laboratories, Las Vegas, Nevada

Open-File Report 98-461

Prepared in cooperation with the U. S. Department of Energy Yucca Mountain Site Characterization Project

1998

ABSTRACT

The Crater Flat structural basin, which includes Yucca Mountain, formed on the south flank of the southwestern Nevada volcanic field during a pulse of rapid extensional deformation having a tilting-domino structural style. The percentage of extension in the basin ranges widely with the method of estimation, at least from 30 to 70%. Nonetheless, the pattern of change in extension rate from the middle Miocene to the present is clear because the magnitudes of the changes in extension rate through time far exceed the magnitudes of the uncertainties associated with the estimates of these rates. During the major pulse of extension that initially formed the basin, between 12.7 and 11.6 Ma, the basin extended 18 to 40% (about two-thirds of the total extension in the basin) in 1.1 m.y. or less. After 11.6 Ma, the rate of extension in the basin declined in a roughly exponential manner, and the late Quaternary rate of extension is less than 1% of the initial rate.

The opening of Crater Flat basin has been strongly oblique, with the least cumulative extension (about 7 to 15%) and the least vertical-axis rotation (less than 5°) in the northeast part of the basin, on north Yucca Mountain. From there, the magnitude of deformation increases to the west and south, to maximum values of at least 50 to 100% extension and at least 45° clockwise rotation in the southwest corner of the basin. The areal variation in vertical-axis rotation in Crater Flat basin closely follows the variation in magnitude of extension suggesting that the rotation is related to the extension as a consequence of fan-like opening of a pull-apart basin and as a related element in transtensional deformation.

Basalts have erupted in the Crater Flat basin in four episodes that together define a trend of progressively declining volume of magma erupted over time. Vents for these eruptions form a northwest-trending alignment across the southwest part of the basin, coincident with the strongest transtensional deformation in the basin, suggesting that ascent of basalt through the crust is structurally controlled.

The rates of extension, vertical-axis rotation, and volcanism in the Crater Flat basin all define initial peaks in activity in the Miocene, followed by strongly declining patterns to the present. The similarity and approximate synchroneity of these trends suggests that all three are

reflections of a single phenomenon -- a tectonic system that, at its peak, must have been the one of the most active zones of tectonism in the Great Basin, comparable to Death Valley today. The Crater Flat basin remains tectonically active, but is now in a very advanced stage of decline. However, the current pattern of deformation in this basin, as reflected in Quaternary fault slip data, still mimics the original fan-like pattern of basin opening established during the episode of peak tectonic activity in the Miocene. Existing data suggests that, within the overall declining pattern, extensional faulting activity has risen and fallen cyclically, and that it varies partly in concert with episodic volcanism in the Crater Flat basin.

INTRODUCTION

Past and ongoing geologic and geophysical studies have delineated the tectonic and volcanic history of Yucca Mountain and the surrounding Crater Flat structural domain. The majority of these data were collected by scientists of the U. S. Geological Survey, the Los Alamos National Laboratories, and the University of Nevada. Many of the investigations were specifically designed to provide the data required for seismic and volcanic hazards assessments of the potential high-level radioactive waste repository site at Yucca Mountain.

The purpose of this paper is to quantitatively synthesize the data concerning the evolving spatial patterns of extensional tectonism, vertical-axis rotation, and volcanism in the Crater Flat basin, from the initial formation of this basin, at about 12.7 Ma, to the present. The structural and stratigraphic framework of the Crater Flat basin and adjacent structural domains are briefly summarized; greater detail is in a companion paper by Fridrich (1998).

CRATER FLAT BASIN

The Crater Flat basin is an asymmetric graben on the south flank of the southwestern Nevada volcanic field, in the southwest Great Basin (Fridrich, 1998). The Crater Flat domain is part of a mosaic of structural domains that comprise the Walker Lane belt, a 100-to-300-km-wide by 700-km-long zone of irregular topography and discontinuous strike-slip structures between the

Sierra Nevada and the northern Basin and Range province (Stewart, 1988).

Like other structural domains in this region, the Crater Flat basin is bounded by structures across which there are abrupt, fundamental changes in the style, timing, and magnitude of extension and other deformation, and of magmatism (Fridrich and others, 1996; Fridrich, 1998). The western boundary of the Crater Flat basin is the Bare Mountain range-front fault (Figure 1). The northern boundary consists of a gradational termination of intrabasin structures at the perimeter of the Timber Mountain caldera complex. The northeastern boundary is drawn along Yucca Wash (Figure 1), a linear valley which is inferred to be underlain by a small accommodation zone separating the northeastern part of basin (north Yucca Mountain) from a more strongly extended domain to the northeast. The eastern and southern boundaries of the Crater Flat basin are covered by recent alluvium. The locations of the inferred structures that form these boundaries have been interpreted primarily from geophysical evidence (Figure 1; Fridrich and others, 1996; Fridrich, 1998).

Internal Structure

Crater Flat basin is characterized by an array of closely spaced, small to moderate size extensional faults striking into the western range-front boundary (Figure 1). In areas of bedrock exposure, only a narrow (0.5-to-2-km-wide) zone along the westernmost edge of the basin is dominated by intrabasin faults that are synthetic to the range-front fault and by stratal dips westward into the range front. Exposed stratal dips in the rest of the basin, with few exceptions, reflect eastward or southeastward tilting, which is consistent with the down-to-the-west (or -northwest) faults that dominate most of the basin (Fridrich, 1998).

Gravity and seismic refraction surveys indicate that the Crater Flat basin is deepest on the west (Snyder and Carr, 1984; Ackermann and others, 1988; Brocher and others, 1996), and this interpretation is supported by stratigraphic thickening to the west observed in exposures of the Miocene volcanic rocks across the north and south parts of the basin. The greatest local thickness of volcanic basin fill, as well as the largest offsets of faults and stratal dips in the basin are exposed along the west half of a ridge that forms the southern margin of the Crater Flat

physiographic feature. This zone of maximum extension probably extends to the north and south, and may include much and perhaps all of the area of the alluvial flat to the north (Figure 1).

Normal faults within the Crater Flat basin strike northerly in the northeast part of the basin, but change to increasingly northeasterly to the south and west across the basin (Figure 1). In general, the fault pattern within Crater Flat basin is roughly radial to the caldera complex to the north, and curved from north to south across the basin. Stratal tilts increase strongly to the west and south from an area of minimum tilts in the northeasternmost part of the basin, on north Yucca Mountain. The magnitude of extensional faulting also increases to the west and south from north Yucca Mountain, due to decreased spacing between the intrabasin faults and to increased average throw of the major faults.

Time-Stratigraphic Record

The Crater Flat basin formed during the height of eruptive activity in the southwestern Nevada volcanic field. The tectonism that occurred in the basin during emplacement of the major eruptive units of the volcanic field is recorded by features such as angular unconformities, stratigraphic burial of fault scarps, and abrupt changes in thickness of volcanic units across faults. The best control on the structural evolution of the basin is provided by voluminous ash-flow tuffs because these widespread sheets buried much preexisting topography. The tops of the voluminous welded tuff sheets and compaction foliations within them can be used as paleohorizontal indicators, with appropriate precautions, as described below.

The Crater Flat basin is a structural feature that cuts across the grain of older (pre-13 Ma) structural features in the region (Fridrich, 1998). At least some of the structures that comprise this basin evidently were in a nascent stage of formation during the series of eruptions that formed the tuffs of the 12.8-to-12.7-Ma Paintbrush Group (W. Day and C. Potter, USGS, written commun., 1996; Fridrich, 1998). The basin then rapidly took shape in a pulse of tectonic activity that culminated between 12.7 and 11.6 Ma. The youngest widespread unit of the Paintbrush Group, the 12.7 Ma Tiva Canyon Tuff, is therefore the oldest time-stratigraphic unit of interest in this study. Estimates of the total extension and total vertical-axis rotation that have occurred

in Crater Flat basin, as discussed below, are based on the deformation of the Tiva Canyon Tuff in the Crater Flat domain.

The next younger units of interest are those of the Timber Mountain Group which, in Crater Flat basin, are represented by the 11.7-to-11.62-Ma rhyolite of Fluorspar Canyon (bedded tuffs) and the 11.6 Ma Rainier Mesa Tuff, both of which are widespread, and by the 11.45 Ma Ammonia Tanks Tuff (Sawyer and others, 1994), which is only locally present and exposed. The angle of discordance between the Timber Mountain units in Crater Flat basin and the underlying Tiva Canyon Tuff is the basis for estimating the rate of extension in Crater Flat during the initial 1.1 million years of the basin's tectonic history, between 12.7 and 11.6 Ma.

The next interval for which most of the deformation in the basin can be estimated is from 11.6-to-10.5 Ma. The stratigraphic units that provide the younger limit for this interval are the oldest basalts in the basin, which were erupted at about 10.5 Ma (Swadley and Carr, 1987) and rock-avalanche breccias which are locally exposed and locally encountered in the subsurface on the west side of the basin. These breccia sheets are also roughly 10.5 Ma in age; in different locales where both units are present, the breccias are found either overlying and underlying the 10.5 Ma basalts (Swadley and Carr, 1987; Carr and Parrish, 1985). In the northwest part of the basin, where the 10.5 Ma basalts are absent, the breccias are composed of 11.6 Ma Rainier Mesa Tuff and are overlain by an ashfall tuff dated at 10.3 Ma. The 10.5 Ma stratigraphic units are confined to western part of the basin; however, the majority of the post-11.6 Ma deformation in the basin occurred in this western area. The 10.5 Ma stratigraphic units therefore constrain the majority of the 11.6-to-10.5 Ma deformation.

From 10.5 Ma to present, the stratigraphic units deposited in Crater Flat basin are dominantly alluvial basin-fill deposits, most of which are poorly exposed and difficult to date. Hence, the record of extensional tilting of strata over time can be used only to constrain a single estimate of the magnitude of extension for the entire interval from 10.5 Ma to the present. However, abundant fault-offset data for the late Quaternary in Crater Flat basin allow another estimate to be made, using a different methodology, of recent extension, as discussed below.

DATA SYNTHESIZED IN THIS STUDY

Geologic Map Data

The major information used in this study for calculating the spatial and temporal patterns of extensional deformation in Crater Flat basin comes from geologic maps. These data include maps of northern and southern Yucca Mountain, on the east side of the Crater Flat basin (Scott and Bonk, 1984; R. B. Scott, USGS, written commun., 1995), a map of the central part of the basin (Faulds and others, 1994), and maps of the northwest and southwest parts of Crater Flat basin that were completed during the present study. The major data extracted from these maps for calculating the magnitude of extension are the tilts of dated volcanic units (Fridrich, 1998). The geologic map data were also used as a basis for constructing cross sections as discussed below. Detailed maps of Pliocene and Quaternary basalts of Crater Flat (see compilation in Crowe and others, 1995) were used as the basis for estimating the volumes of individual eruptive units.

The majority of stratal tilt measurements used in this study are strikes and dips of compaction foliation in ash-flow tuffs. These foliations are less reliable as paleohorizontal indicators than are bedding attitudes because compaction foliation may acquire a primary dip if a tuff welds against a nonhorizontal surface or, more importantly for this paper, if it flows after it begins to weld (Chapin and Lowell, 1979). In several parts of the Crater Flat basin, we compared stratal tilts measured from compaction foliations with those measured from bedding in the same stratigraphic sections. These comparisons show that the dips of compaction foliation and of bedding are generally comparable, but the dips of compaction foliation commonly are steeper on average, especially in the upper part of the Tiva Canyon Tuff in certain parts of the basin (W. Day and C. Potter, USGS, written commun., 1996). In the most notable examples, compaction foliations become steeper upsection through the Tiva Canyon Tuff, in some cases

abruptly steepening upward across a horizon with flow lineations. The generalized values of stratal tilts in different parts of the Crater Flat basin used in this study are all average values, each one derived from ten or more individual field measurements (a more-detailed synthesis of the raw data is shown in Figures 9 through 12 of Fridrich, 1998). Some localized anomalously steep dips were excluded in deriving these averages in an effort to produce values that reflect structural tilting alone.

Quaternary Fault-Slip Data

Detailed studies of Quaternary faults in the Crater Flat basin have included examination of nearly all of the exposed faults in the basin with displacements greater than 30 m. The faults that show signs of Quaternary activity were mapped in detail throughout their exposed lengths, with an emphasis on documenting evidence of recent offset (Simonds and others, 1995). These wide-ranging field studies were augmented by trenching across key localities along these major faults, and by detailed logging of the trenches (Klinger and Anderson, 1993; Menges and others, 1994; Pezzopane and others, 1994; Whitney and coworkers, written comm., 1996).

The Quaternary fault studies in the Crater Flat basin have been supported by geochronologic studies of offset surficial deposits (E. Taylor, USGS, written comm., 1996). The two data sets, in combination, yield estimates of rates of late Quaternary offset along all of the major faults, as discussed below.

Paleomagnetic data

The areal variations in directions of remanent magnetizations from the 11.45-Ma Ammonia Tanks Tuff, 11.6-Ma Rainier Mesa Tuff, 12.7-Ma Tiva Canyon Tuff, and 13.25-Ma Bullfrog Tuff were used to investigate the rotation of fault blocks about steeply inclined axes within the Crater Flat domain. This study includes data from 16 new paleomagnetic sites from the western part of the domain in addition to 45 sites previously reported by Rosenbaum and others (1991) and Hudson and others (1994). The paleomagnetic samples were collected and processed using

methods described in Hudson and others (1994). A full data table of the results is available from M. R. Hudson upon request. Stratal attitudes used for tilt corrections of the paleomagnetic data were derived from numerous measurements of compaction foliation under the presumption that compaction foliation was horizontal when tuffs acquired their magnetization. To detect vertical-axis rotations, declinations of tilt-corrected site mean magnetization directions were compared to reference directions for each unit given by Hudson and others (1994). Tilt-corrected magnetizations directions for four newly acquired sites have inclination discordances that differ by more than 10° from those of expected directions. These inclination discordances may arise at least partly from inaccurate tilt corrections and thus the associated declination discordances may not fully reflect vertical-axis rotation. Nonetheless, the declination discordances for these sites are generally similar to those from nearby sites.

ESTIMATING EXTENSION RATES

Extension in Crater Flat basin was estimated using three different methods: (1) extension in the Miocene bedrock was estimated primarily by using the amount of stratal tilting as a measure of extension, assuming a tilting-domino model; (2) where data permitted, the above estimates were checked using reconstructions of cross sections drawn perpendicular to the average strike of extensional faults; and (3) late Quaternary extension was estimated by summing the horizontal components of Quaternary fault displacements along transects perpendicular to the strikes of major extensional faults. The different methods were employed because bedrock is not well enough exposed in many areas in the Crater Flat basin to construct accurate cross sections; the amount of stratal tilting was thus the only information available on a sufficiently widespread basis to make basin-wide estimates of Miocene extension, and for making estimates for multiple time intervals in individual areas. For the Quaternary extension, the fault slip data derived from trench studies are the only data available on which to base estimates.

All three methods for estimating the percentage of extension require that certain assumptions be made. The most important of these is the deep, subsurface geometry of the extensional faults, which has two components. One is whether the faults are planar or listric or

something in between. In the tilting domino model, the faults are strictly planar by definition. For the reconstructed cross-section method, a range of geometries was considered, as discussed below.

The second component of fault geometry is the assumed initial dip of extensional faults. An average initial dip of 65° was used for all intrabasin normal faults because it is the maximum common value of the dip of normal faults determined from seismological data (multiple fault-slip foci determining a fault plane) in the southern Great Basin including the Yucca Mountain area (Harmsen, 1994; Harmsen and Bufe, 1992; K. D. Smith and J. Brune, University of Nevada-Reno, written commun., 1995). Moreover, fault-to-bedding angles in pre-extensional rocks in the more deeply eroded parts of the Yucca Mountain region commonly range between 60° and 70°. For purposes of this study, the Bare Mountain range-front fault was assumed to have a dip of 60° throughout its history and not to have been tilted as it moved.

A second assumption that must be made is the critical angle of tilting at which original faults are abandoned and a new set of faults form to accommodate further extension and related tilting. As extension progresses, extensional faults are tilted along with the intervening rocks, and the cohesive strength of the faults increases as their dips decrease. At a critical angle, the cohesive strength of the existing fault reaches a value that exceeds the cohesive strength of unfaulted rock at the dip-angle of maximum shear stress (65°), causing a new set of high-angle faults to form (Nur and others, 1989). Field evidence in the Crater Flat basin suggests that the critical angle of tilting in this area is about 25°; most areas having greater than 25° of tilt have a significantly more complex faulting pattern than those with less than 25° of tilt, as would be expected if a second generation of faults had formed. Seismologic evidence (Harmsen, 1994) may support this assumption; 40° is at the lower limit of common values for seismologically determined dips on active faults in the Great Basin.

Our third major assumption concerns how vertical-axis rotation affects extension. We assumed that extension is accomplished by normal faulting and related tilting, and should be calculated along profiles that are perpendicular to the strikes of the major extensional faults. In fact, existing data indicate that this last assumption is not strictly accurate. The lateral changes in the magnitude of vertical-axis rotation across the Crater Flat basin constitute a pattern of

oroclinal bending. The most notable structural feature that accommodates this bending is a widespread set of relatively short, mostly northwest-striking right-oblique normal faults that form bridging patterns between the major north- to northeast-striking normal faults. These bridging faults reflect a secondary (northeast-southwest) pattern of extension that is roughly orthogonal to the primary direction of extension (W. Day and C. Potter, USGS, written comm., 1996; Minor and others, 1996). Based on existing data, this secondary component of extension is trivial in magnitude relative to the primary northwest-southwest extension. Because we ignored this secondary component, our estimates of percent extension are slightly low. However, the magnitude of this effect is probably less than the degree to which the tendency for compaction foliations to be steeper than the true degree of stratal tilt leads to overestimation of the percent extension.

The first two assumptions above, which concern fault geometry and how it evolves with progressive deformation, are much more of a concern because they may significantly change the estimates if they are inaccurate. However, these assumptions fortunately affect all three methods for estimating the magnitude of extension in a similar manner, and roughly to the same degree. Hence, the lack of complete confidence in these assumptions creates uncertainty principally in the absolute value of the estimates of the magnitude of extension. Because of the consistency in making the same assumptions throughout, there is much less uncertainty in relative values. Hence, the estimates made using the three different methods are generally comparable to one another, and the estimates for different time intervals using any one methodology are also comparable. This relationship is important for achieving the goal of this study, which is principally to determine the pattern of change in the extension rate through time, rather than the absolute amount of extension.

Of the three methods employed for estimating percent extension, only the one based on tilting requires mathematical definition, the tilting-domino model. For this purpose, the equation presented by Nur and others (1989) was applied:

Elongation = l/l_0 = sin α divided by sin (α - θ)

where:

α = initial fault dip = 65°

θ = stratal tilt

% extension = $100[l/l_0 - 1]$

l = measured length

l_o = original length

Extension Rates Based on Domino Model

Extension rates are initially estimated using stratal tilts and the equation of Nur and others (1989). As explained below, these initial estimates are considered to be "maximum" values, or at least upper-range estimates. The initial estimates were then qualified by comparison with those derived using the reconstructed cross-section method, and a complementary suite of "minimum" (lower-range) estimates were generated based on that analysis. Finally, an estimate of the late Quaternary extension rate was made based on fault-slip data from trench studies. All of the estimates were then collated and plotted against time to show the estimated pattern of changes in extension rate in the Crater Flat basin from the middle Miocene to the present. For all of the estimates below, the southernmost part of the Crater Flat basin was not included owing to the absence of control (total alluvial cover) in that area.

Estimates of extension rates both higher and lower than those here could, no doubt, be made if additional conceptual models of the process of extension were entertained. Our "maximum" and "minimum" estimates are intended to bracket the most probable range of the the magnitude of extension in the Crater Flat basin.

Extension Rate From 12.7 to 11.6 Ma

The first interval for which extension rates are estimated corresponds to the initial extensional pulse that created the Crater Flat basin between 12.7 and 11.6 Ma. The basin-wide

variation in the tilt of the 12.7 Ma Tiva Canyon Tuff, corrected for the post-11.6 Ma tilt of the Rainier Mesa Tuff (Figure 2A) is based on map data (see Fridrich, 1998). The variation in corrected tilt is shown by dividing the basin into a series of tilt domains each assigned an average value (Figure 2A). The basin-wide variation in the percentage of extension for the 12.7-to-11.6 Ma interval (Figure 2B) was calculated from these corrected tilts. These estimates, made using the domino model, are considered to be maximum values; complementary minimum values, discussed below, are shown in parentheses.

Some elements of the data used in constructing the above estimates (Figure 2) are interpretative. For example, the area with 30° of tilt (Figure 2A) is an area with no exposure of Tiva Canyon Tuff; we extrapolated the trend of westward increase in angular discordance between Tiva Canyon Tuff and Rainier Mesa Tuff, documented in the exposures to the east and north, into this area.

For the Bare Mountain fault, along the west margin of Crater Flat basin, we know only the total offset for the interval from 12.7 Ma to present. We interpretively divided the total offset among the 12.7-11.7-Ma, 11.7-10.5-Ma, and 10.5-Ma-to-present intervals based on two lines of evidence. First, all of the basin-filling (post-12.7-Ma) units in Crater Flat basin thicken strongly westward, toward the Bare Mountain fault, especially the units of the Timber Mountain Group (Fridrich, 1998). We interpret this stratigraphic thickening of basin fill toward the Bare Mountain fault as a reflection of activity on this fault. If so, then the extent of thickening of different-age units toward this fault indicates that the most active period of displacement on the range-front fault was between 12.7 and 11.6 Ma, and that activity on this fault then declined strongly and progressively with time.

The above interpretation is supported by the second line of evidence, which concerns the ages of emplacement of rock-avalanche breccias in the basin that were shed from the eastern range front of Bare Mountain, and from the east flank of the Tram Ridge domain to the north. We interpret the rock-avalanching as resulting from a combination of creation of an oversteepened range-front scarp and from active seismicity on the range-front fault. The rock-avalanche breccias are thus indicators of the most active periods of tectonism on the range-front fault. These breccias are of two age groups; the larger-volume group was emplaced between 12.7 and 11.6 Ma, and the

smaller-volume one was emplaced between 11.6 and 10.5 Ma (Fridrich, 1998). Both the pattern of thickening of basin fill toward the range-front fault, and record of rock avalanching off the range front thus support our interpretation that activity on the range-front fault peaked between 12.7 and 11.6 Ma, with more than 50% of the total displacement having occurred in that 1.1 m.y. period, and the rate of displacement declined exponentially from 11.6 Ma to the present.

The specific estimate of 1500 m of horizontal offset on the southern part of the Bare Mountain fault (3 km of displacement on a 60° fault; Figure 2A) is based on the fact that the rock-avalanche breccias shed off Bare Mountain between 12.7 and 11.6 Ma are composed almost entirely of Paleozoic rocks (Carr and Parrish, 1985). These rocks evidently were covered by at least 2 km of Tertiary section immediately before the Crater Flat basin and the Bare Mountain uplift initially formed between 12.7 and 11.6 Ma (Fridrich, 1998). Hence, the Bare Mountain fault incurred a vertical offset of at least 2 km in that interval just to expose the Paleozoic rocks. The Tertiary rocks are largely absent from the rock-avalanche breccias because the Paleozoic rocks of Bare Mountain were tectonically denuded of their Tertiary cover from both sides of the uplift during the same (12.7-11.6-Ma) extensional pulse. Supporting evidence for this interpretation has been supplied by Hoisch and others (1997) who infer from thermochronologic data that the Paleozoic and latest Precambrian rocks of Bare Mountain were rapidly uplifted from several kilometers depth to less than 1 kilometer depth at approximately 12 Ma.

The above analysis yields an estimate of the magnitude of extension within the Crater Flat basin (the upper plate), which averages 30% over the area of the basin for the 1.1 m.y. interval. The basin is depicted as the "upper plate" because it is the hangingwall of the Bare Mountain range-front fault, which we view as being the "master fault" of the basin. The east flank of the Bare Mountain uplift is thus the "lower plate" below the master fault, and tectonic denudation of the lower plate, by movement along the range-front fault, is seen as an additional component of the extension associated with the creation of the Crater Flat basin.

Ideally, we would also include movement along the Gravity fault (GF, Figure 6), the eastern boundary of the basin, in the total extension; however, there are insufficient data on this largely buried fault to include it. Because the Gravity fault is significantly smaller than the Bare Mountain fault, the failure to include it results in only a small underestimation of the total

extension involved in creation of Crater Flat basin.

The horizontal component of slip on the Bare Mountain fault is shown as infinite extension over the affected area because this is the area of tectonic denudation of the Paleozoic lower plate; extension of the upper plate in this area is infinite because the upper plate has been completely removed (Figures 2A and 2B). Using the below-determined estimate of the original (pre-extensional) width of the Crater Flat basin, tectonic denudation by itself is responsible for an additional 10% extension in the Crater Flat domain from 12.7 to 11.6 Ma, and the sum of the two estimates is 40%. Dividing 40% total extension by the 1.1 m.y. length of the interval, the extension rate is estimated to have been 36% per million years during the extensional pulse that created the Crater Flat basin.

The inclusion of slip on the Bare Mountain fault in the estimates of extension of Crater Flat basin is model dependent. We assumed that the Bare Mountain fault is a high-angle fault down to the brittle-ductile transition, at about 15 km depth, and that only the tilts in the narrow zone of westward dips in the westernmost part of the basin are related to movement on the range-front fault. A possible alternative model is that the Bare Mountain fault is the surface expression of a listric detachment fault that underlies all of Crater Flat basin. If this fault is a detachment, then the slip along it may be directly related to the tilting throughout the basin and, if so, then we have overestimated percent of extension by including both fault slip and the related tilting in making the estimate. Based on available data, we have intepreted, however, that slip on the Bare Mountain fault declined exponentially after the initial pulse of activity, as discussed above. Because this is the same pattern as is indicated by tilting within the basin, including the slip on this fault will not substantially alter the estimated pattern of change in extension rates through time, and thus will not affect the major conclusions of this paper, discussed below, even if we have erred by including it.

The areal pattern of extension from 12.7 to 11.6 Ma in the Crater Flat basin resembles that of a triangular pull-apart basin, with the minimum percentage of extension in the northeastern part of the basin and progressively increasing percentage of extension to the west and south from that apparent pivot point (Figures 2A and 2B).

Extension Rate from 11.6 to 10.5 Ma

The second interval for which estimates of extension rate are made is from 11.6 Ma, the end of the last interval, to 10.5 Ma, the time of emplacement of the oldest basalts in the basin and of widespread, roughly coeval rock-avalanche breccias (the younger group of breccias discussed above). Significant tilting in this second interval (Figure 3A) was limited to the west side of the basin, where there is control only in confined areas in the southwest and northwest parts of the basin; the rest of the western part of the basin is covered by recent alluvium. The areal pattern of extension shown between these two areas of control is an interpolation and assumes that the northward decrease in magnitude of tilting, and therefore of extension, is gradational between the existing sparse data points (Figure 3B).

East of this distinct zone of extension on the west side of the basin, 10.5 Ma rocks are absent, but the 11.6 Ma Rainier Mesa Tuff is tilted only about 5° on average and most of this tilting is assumed to have occurred by 10.5 Ma. The basis of this assumption is that all other data suggest that the overall pattern in the change in extension rate with time is a roughly exponential decline after the initial 12.7-to-11.6-Ma pulse.

For the 11.6-to-10.5-Ma interval, it is estimated that 11% extension took place within the upper plate as well as an additional 5% extension related to tectonic denudation of Bare Mountain. The total percent of extension for the 1.1-m.y. period is 16% and the extension rate in this interval is 14.5% per million years. These are maximum estimates for the 12.7-to-11.6-Ma interval; minimum estimates, generated below, are shown in parentheses (Figure 3).

The northward decrease in percent of extension in the 11.6-to-10.5-Ma interval (Figures 3A and 3B) is consistent with a triangular pull-apart mechanism of basin opening, as was true for the 12.7-to-11.6-Ma interval. The westward migration of the focus of extension between the 12.7-to-11.6 Ma and the 11.6-to-10.5-Ma intervals is part of a regional pattern of westward migration of the focus of extension that occurred throughout a large part of the Yucca Mountain region from about 12.7 Ma at least to about 8 Ma (Fridrich, 1998). The strong localization of the extension of the 11.6-to-10.5-Ma interval in the west part of Crater Flat basin is the major factor that created the physiographic distinction between Crater (alluvial) Flat and the Yucca Mountain uplift, a

distinction that has survived to the present.

Extension Rate From 10.5 Ma to Present

The third interval for which estimates of extension rate are made extends from 10.5 Ma to the present. The 10.5-Ma rocks in the Crater Flat basin are nowhere tilted more than about 15°; tilts exceeding 5° are found only in the westernmost part of the basin (Figure 2-7A), the area that was also the locus of extension between 11.7 and 10.5 Ma, as discussed above.

For this interval, it is estimated that the upper plate was extended 4.5% (Figure 2-7B) and that an additional 2% extension is associated with movement on the Bare Mountain fault. Total extension for the interval is thus 6.5% and the average extension rate for the 10.5-m.y.-long interval was 0.6%. The southward-increasing pattern of tilting, and therefore of extension, in this interval indicates continuation of the fan-like pattern of extensional basin opening established during the initial formation of the basin (Figures 4A and 4B).

Total Extension from 12.7 Ma to Present

An estimate of the total extension in Crater Flat basin was needed in this study as a basis for including tectonic denudation of Bare Mountain into the extension estimates. The total percent extension within the Crater Flat basin (in the upper plate) was estimated by multiplying the areal distributions of percent extension for the three time intervals above (12.7-to-11.7-Ma, 11.7-to-10.5-Ma, and 10.5-Ma-to-present) and producing a contour map as the result (Figure 5A). The average total percent of extension within the basin is 54%, thus the pre-extensional width of the basin is estimated to have been slightly less than two-thirds of the average current width of the upper plate (24 km), or 15.6 km. Given an average 2 km of horizontal slip along the Bare Mountain fault, tectonic denudation is responsible for about 17% extension across the Crater Flat domain and the total average percent extension is therefore 71%. The average percent extension of the upper plate along the northern and northeastern boundaries of Crater Flat basin is 20% whereas the average percent upper plate extension along the southern part of the basin is about

65% (Figure 5A).

Extension Rates Based on Reconstructed Cross Sections

The percentage of extension in an area can be estimated by constructing a balanced cross section drawn perpendicular to the direction of extension. Estimates determined by this technique vary as a function of the underlying assumptions and interpretations that are used to draw the balanced cross section. For example, if a tilted-domino model is used that assumes perfectly planar faults with initial dips of 65°, the estimated percent of extension by the reconstructed cross-section method is similar to that derived from stratal tilts by the equation of Nur and others (1989; see above).

Numerous data from the Crater Flat basin suggest that the tilted-domino and planar fault model may not be the best assumption for use in this area. If the domino model was strictly accurate, there should be no systematic changes in dip across major fault blocks. However, two types of such changes have been widely observed in this basin (e.g., Scott, 1990; W. Day and others, USGS, written commun., 1995). First, many of the major faults consist of several strands in zones that cut across axially coincident monoclines (Scott, 1990; Fridrich, 1998). This geometric relation suggests that the faults bifurcate and change dip upward. The monoclines in the volcanic section may represent drape over simpler, larger (aggregate) offsets in the underlying Paleozoic sedimentary rocks. Second, many fault blocks show evidence of a pronounced westward increase in dips. The most probable explanation for these variations in dip is that roll-over structures are developed in the hanging walls of the major faults. These apparent roll-over structures suggests that the major intrabasin faults have the form of curved planes; they probably are not truly listric but neither are they strictly planar. At least part of the observed dips of the fault blocks may thus be the result of rotation slip along the slightly curved fault planes.

The consequence of the above factors is that the underlying assumption of the Nur and others (1989) equation -- that tilting is purely a result of domino-style extension -- is not strictly applicable. Roll-over effects cause an overestimation of percent of extension using that equation, and drape effects cause an underestimation. Of the two, roll-over is much the larger effect and

the above estimates of the magnitude of extension may be overestimates, or at least maximum estimates. Thus, to bound the problem, there is a need to generate a complimentary suite of minimum estimates.

In broad fault blocks, the area between the rollover structure and the monoclinal flexure should, in theory, most closely approximate that component of dip that caused by the tilting-domino effect of the Nur and others (1989) equation. In the Crater Flat basin, dips in these areas have a value of at least half, and generally much more than half, of the average dip of the entire fault blocks. Our minimum estimates for the percent of extension in the Crater Flat basin were generated by using half of the average value of the observed dips in the Nur and others (1989) equation, rather than the whole value. Based on our work with balanced cross sections, the assumption that half of the dip results from slip along curved fault planes is appropriate for a listric model of fault geometry; even in a listric model, approximately half of the average stratal tilting results from the tilting domino mechanism. The minimum values generated using the listric model are shown in parentheses on the maps that show the areal distributions of percent extension for the three major time intervals (Figures 2B, 3B, and 4B).

These minimum estimates lead to a change in the estimates for the percent of extension associated with tectonic denudation of Bare Mountain because those estimates are derived by dividing the width of the zone of tectonic denudation by the preextensional width of the basin (the estimated restored width at the time). No change was made in the assumption that the Bare Mountain range-front fault has had a constant dip of 60°. With the minimum estimates of percent extension, the calculated magnitude of extension resulting from tectonic denudation is also reduced (because the estimated preextensional width of the basin is greater); but this reduction in the estimates is not as large as the reduction in the estimates of the within-basin (upper plate) extension.

Recent Extension Rate Based on Quaternary Fault-Slip Data

Fault offsets of deposits ranging in age from about 100 to 900 Ka are used to estimate late Quaternary extension in the Crater Flat basin. The paleoseismic data were collected from more

than 80 trenches and from natural exposures of twelve faults that show evidence of Quaternary movement (Klinger and Anderson, 1993; Menges and others, 1994; Pezzopane and others, 1994; Simonds and others, 1995). Each Quaternary fault studied has experienced two to seven surface ruptures having average vertical displacements of 4 to 160 cm per event (mostly in the range of 20 to 90 cm). Horizontal fault offsets were calculated from the measured vertical offsets assuming fault dips of 60°, 55°, and 50° along the north, intermediate, and south transects, respectively. The horizontal offsets were then converted to horizontal slip rates using the ages of offset surficial deposits, dated by the uranium-series disequilibrium or by volcanic ash geochronology. The collated horizontal-slip rates of the Quaternary faults (Figure 6) illustrate the recent pattern of faulting in the basin, and demonstrate the areal variation in the rates of fault offsets throughout the basin.

These data can be compared to the estimates of Miocene-to-present extension rate by summing the horizontal components of slip rate from each Quaternary fault along three transects (see Figure 6) drawn roughly perpendicular to the extensional fault system. Extension rates along these three transects are 0.025%, 0.1%, and 0.2% per million years from north to south. The overall average extension rate for the Crater Flat basin has been 0.1% per million years during the late Quaternary.

The above estimate of the recent extension rate along the south transect across the basin, is low by an unknown but probably small amount because we have no data on the gravity fault (GF; Figure 6). The gravity fault is known to have slipped in the Quaternary because scarps of this fault cut Pleistocene alluvial fans in the southeastern part of the Crater Flat basin (D. O'Leary, USGS, oral comm., 1996). However, these scarps are subtle features, which suggests that the recent slip rate on this fault is no greater than that of the major intrabasin faults to the east of it.

A low Quaternary slip rate of 0.01 mm per million years on the Bare Mountain fault presents an apparent paradox in the Quaternary evolution of the Crater Flat basin. A tectonic study of alluvial fans on the east side of Bare Mountain suggests that recent subsidence is greater at the south end of Crater Flat than to the north (Ferrill and others, 1996). Moreover, burial of the middle Quaternary (1 Ma) basaltic centers of Crater Flat (Figure 1) increases to southwest; the southwesternmost center has been buried by about 30 m of alluvium, whereas the northeasternmost

one apparently has not been buried significantly. Based on this evidence, J. Stamatakos (Southwest Research Institute, written commun., 1996) has suggested that a higher rate of faulting on the southern part of the range-front fault, relative to the northern part, is responsible for the increase in recent sedimentation in the south.

If so, then the southern part of the Bare Mountain fault may be more active than recent studies suggest, perhaps because recent sedimentation in southwestern Crater Flat has hidden some strands of the range-front fault. Gravity models in fact suggest that the major strand(s) of this fault are located east of the exposed trace, under late Pleistocene alluvium (V. Langenheim, USGS, written commun., 1994). The estimate of recent extension rate along the southern transect across Crater Flat may thus be too low by as much as a factor of nearly two, and the estimate of recent extension rate for the whole basin may thus be low by as much as 50%. The above estimate of extension rate of 0.10% per million years is thus a minimum estimate; our maximum estimate is 0.15% per million years (Figure 7A).

The areal variation in the pattern of late Quaternary extension in the Crater Flat basin, as shown by the differences among the three transects, is one of strong southward increase in deformation rate. The original fan-like pattern of basin opening established in the Miocene still persists. This continuing pattern of oblique basin opening indicates that vertical-axis rotation must still be occurring at a rate that is significant relative to the rate of extension.

Overall Pattern of Extension Rates Through Time

To show the pattern of change in extension rate during the evolution of the Crater Flat basin, the range of estimates of extension rates for each interval are plotted against time (Figure 7A). A number of uncertainties are associated with these estimates, including those associated with comparing estimates derived using the different methods, and those that are inherent in the interpretative assumptions that were used in making the estimates. Nonetheless, the trend established by the data is clear because the magnitude of change in extension rate over time far exceeds the magnitude of uncertainty associated with the estimates. The pattern is an exponential decline from the initial pulse which formed the basin (Figure 7A; also see Carr, 1984).

Importantly, the estimates of the Quaternary extension rate fit the overall trend of the change in extension rate since the middle Miocene. The maximum estimate of the late Quaternary extension rate is less than 1% of the minimum estimate of the initial (12.7-to-11.6-Ma) extension rate in the Crater Flat basin.

VERTICAL-AXIS ROTATIONS IN CRATER FLAT BASIN

Paleomagnetic data indicate that the curved pattern of faults on the east side of the Crater Flat basin is due to southward-increasing clockwise rotation (Rosenbaum and others, 1991; (Hudson and others, 1994; Figure 8). Preliminary paleomagnetic data collected in the northwest part of Crater Flat suggest that the observed radial pattern of faults around the caldera complex is partly a primary feature, but has been accentuated by westward-increasing clockwise rotation across the northern part of the basin. Thus the variation in the strikes of faults within Crater Flat basin (Figure 1) not only largely reflects the pattern of vertical-axis rotation in the basin but it also reflects localized modification of the regional stress field near the caldera complex at the north boundary of the basin (Christiansen and others, 1965; Cummings, 1968).

Within the Crater Flat basin, a northwest-trending "hinge-line" can be defined that separates an area of predominantly north-striking faults, on the northeast, from an area of predominantly northeast-striking faults, on the southwest (Figure 1). Fault strikes in the north and south parts of the basin are based on mapping (e.g., Scott and Bonk, 1984; R. B. Scott, USGS, written commun., 1995), whereas in the central area which is largely covered by Quaternary alluvium and Plio-Pleistocene basalts, existing field data (Faulds and others, 1994; Simonds and others, 1995) were augmented by aeromagnetic data. Abundant narrow linear aeromagnetic anomalies are present in this basin (Grauch and others, 1993); these anomalies principally reflect fault offsets of the highly magnetic Topopah Spring Tuff and allow tracing of major faults through many areas of alluvial cover (V. Langenheim, USGS, oral commun., 1995).

The hinge-line corresponds approximately to the contour of 20° clockwise rotation of the Tiva Canyon Tuff; greater than 20° dextral rotation is present southwest of this line and less than 20° rotation is present northeast of the hinge-line, in general (Rosenbaum and others, 1991;

Hudson and others, 1994; compare Figures 1 and 8). A subtle but abrupt decline in average elevation (lower on the southwest side) is present across the hinge-line along most of its length, reflecting a southwestward increase in the magnitude of extension. Most faults that cross the hinge-line show a pronounced southward increase in both Quaternary displacement and total bedrock displacement across it (compare Figures 1 and 6; Scott and Bonk, 1984; Menges and others, 1994; A. Ramelli, NBMG, oral commun., 1995).

Whereas paleomagnetic data indicate that vertical-axis rotation changes gradationally across most of the basin (Figure 8), field relations along the hinge-line indicate that, within that gradient, a step increase in extension and distibuted strike-slip deformation (vertical-axis rotation) is present across this line, with greater deformation to the west than to the east. The paleomagnetic data show the step change in the northern part of the basin (Figure 8) and, given uncertainties in the data, are permissive of a smaller step change to the south as well. The zone of strong vertical-axis rotation extends to the Bare Mountain fault system, and the Rainier Mesa and Ammonia Tanks Tuffs are significantly less rotated immediately west of this domain-bounding fault than they are to the east of it (Figure 8).

The paleomagnetic data from the Crater Flat basin show that older units are rotated more than younger ones (Figure 8). The difference in degree of rotation between the 13.25 Ma Bullfrog Tuff and the 12.7 Ma Tiva Canyon Tuff is slight, and probably not statistically significant given the small number of measurements in the Bullfrog Tuff. Curiously, the average rotation of the Tiva Canyon Tuff is only 10-20% more than the 11.6 Ma Rainier Mesa Tuff, indicating that the major pulse of vertical-axis rotation in the Crater Flat basin did not coincide with the major pulse of extension, but rather followed it (Hudson and others, 1996). The Rainier Mesa Tuff is significantly more rotated than is the 11.45 Ma Ammonia Tanks Tuff. These two units therefore closely bracket the onset of major rotation, the peak of which probably followed the peak in extension rate by about 1 m.y. (Hudson and others, 1996).

The number of data points is fairly low for the Rainier Mesa and Ammonia Tanks Tuffs, so there is some uncertainty associated with the above conclusions. However, the basic pattern described by the data is an abrupt peak in clockwise rotation followed by a rapid decline. The similarity of this pattern to the well-documented patterns of extension and volcanism in the basin

(Figures 7A and 7B) suggests that the basic pattern described by the paleomagnetic data is accurate.

The areal variation in vertical-axis rotation in Crater Flat basin closely follows the variation in magnitude of extension (compare Figures 6 and 8) suggesting that the rotation is related to the extension as a consequence of oblique opening of the basin (fan-like opening of a pull-apart basin) and as a related element in transtensional deformation.

BASALTIC VOLCANISM IN CRATER FLAT BASIN

The southwestern Nevada volcanic field began to form between 16 and 15 Ma, and culminated between 12.8 to 11.4 Ma in four especially voluminous silicic ash-flow eruptions (of about 1000 km^3 of magma apiece; Sawyer and others, 1994). The youngest silicic centers of the field formed between 9.5 and 7.5 Ma and consist of two calderas that were the source of relatively small-volume ash flow eruptions, and several rhyolitic dome fields. This waning phase of the silicic volcanic activity was marked by the onset of large-volume basaltic volcanism that was temporally and spatially associated with the calderas. Younger (post-7.5-Ma) activity in the volcanic field was largely if not entirely basaltic and became progressively clustered into ever fewer and smaller discrete zones. One of only two Quaternary zones of volcanism in the southwestern Nevada volcanic field is located in the Crater Flat basin, where basalt has erupted in four episodes that together define a trend of decreasing volume of magma erupted over time (Figure 7B).

Individual vents for the four basaltic eruptions are mostly northeast-striking (Fridrich and others, 1994; Crowe and others, 1995), although northwest-striking dikes are also common, particularly on north Yucca Mountain. The dominant northeast strikes probably reflect preferential dike emplacement perpendicular to the least principal stress, which had a northwest orientation during most of the history of the Crater Flat basin (Minor and others, 1996). The deviation of some of the dikes from being perpendicular to the least principal stress direction may result from a number of physical effects including localized modification of the stress field by dike emplacement itself during injection of a series of dikes (Parsons and Thompson, 1991) as well as

emplacement of dikes along preexisting weaknesses. The large subpopulation of northwest-striking dikes suggests that northwest-striking structures (which in this basin are predominantly right-slip structures) may preferentially act as high-level pathways for magma ascent.

On a larger scale, the major basaltic centers in Crater Flat basin are aligned across the southwest part of the basin. This northwest-trending alignment of the majority of the vents is coincident with the zone of greatest transtensional deformation in the Crater Flat basin, which lies between the hinge-line of the basin and the Bare Mountain fault (Figure 1). The only vents that do not define this alignment are a cluster of about twelve dikes on northern Yucca Mountain, which form a secondary alignment, also northwest-trending, within a transtensional zone associated with the northwest-striking strike-slip faults on northern Yucca Mountain (Figure 1). Alignment of the two groups of basaltic vents along the two major transtensional zones within the basin suggests that these zones controlled the ascent of basalt through the upper crust. Of these two clusters of vents, only the one in western Crater Flat basin is currently active; the one on northern Yucca Mountain was active only in the 11.3-to-10.5-Ma episode and is evidently extinct.

An important implication of this study with respect to volcanic hazards for the Yucca Mountain site is that basaltic volcanism has, since the late Miocene, been restricted to the transtensional zone in western Crater Flat basin. This relation suggests that volcanism on north Yucca Mountain is significantly less likely than predicted by previous models (Crowe and others, 1982; Smith and others, 1991; Connor and Hill, 1995; Geomatrix Consultants and TRW, 1996). The potential repository site on north Yucca Mountain lies well outside the transtensional zone along which post-Miocene basaltic vents are concentrated.

EPISODIC TECTONIC ACTIVITY IN CRATER FLAT BASIN

An important question for seismic hazards assessment at Yucca Mountain is whether faulting in Crater Flat basin fluctuates significantly with time. Two lines of evidence suggest that seismic activity varies episodically.

Evidence of Episodicity from Breccias and Basalts

Rock-avalanche breccias of the Crater Flat basin fall into two age groups. The older group was emplaced between 12.7 and 11.6 Ma, during the major pulse of extension that formed the Crater Flat basin (Fridrich, 1998). A second group of rock-avalanche breccias are roughly contemporaneous with the 10.5 Ma basalts of the basin, as discussed above, indicating that this first and major pulse of volcanism in the basin (Figure 7B) was also a time of heightened seismic activity. The implications of this second group of breccias are: (1) that within the overall exponential declining pattern (Figure 7A), extensional faulting activity in the Crater Flat basin has risen and fallen episodically, and (2) that the episodicity in faulting activity has occurred at least partly in concert with the episodicity in volcanic activity in the basin.

Moreover, the 10.5 Ma basalts of the Crater Flat basin are concentrated in a thin zone in the southwesternmost part of the basin, which was a zone of focused extensional faulting in the 11.7-10.5 Ma interval immediately prior to eruption of these basalts (compare Figures 1 and 3). This suggest that there may be both a temporal and a spatial correlation between focused pulses of faulting and of volcanism in the basin.

These implications are supported by field relations of the 3.7 Ma and 70 ka basalts of Crater Flat basin. The 3.7 Ma basalts consist mostly of thin (typically 1-3 m thick) flows erupted from a north-trending fissure-vent system. The distribution of these lavas indicates that the basalt flowed almost exclusively eastward from the fissure vent system toward the scarp of the Windy Wash fault (see Figure 12 of Fridrich, 1998). Against the scarp of this fault, the basalts overlie fine-grained sediments. Individual lava flows locally attain thicknesses of 10-30 m immediately downthrown against this fault scarp, indicating that the lavas ponded in a local depression. The evidence of a paleodepression immediately downthrown on the Windy Wash Fault suggests that this fault was very active immediately prior to the emplacement of the 3.7 Ma basalts, at least in the vicinity of the 3.7 Ma basaltic center.

The 70 ka basalt (the Lathrop Wells cone; Crowe and others, 1995) is located between the southern ends of the Windy Wash and Stagecoach Road faults (compare Figures 1 and 6). The southern ends of these two faults were the most active sites of faulting activity in the late

Quaternary in the Crater Flat basin (Figure 6). Moreover, in the case of both of these faults, slip rates during the late Pleistocene exceed the average rate of fault slip over the last 8 m.y. (for example, see the discussion below of the Stagecoach Road fault). The 70 ka basaltic center is thus spatially coincident with the site of strongest tectonism in the Crater Flat basin in the late Quaternary and, moreover, existing evidence suggests that creation of this basaltic center has been temporally coincident with a pulse of heightened faulting activity in this area.

Evidence of Episodicity from Fault Studies

A reworked pumice unit exposed in a trench on the footwall of the Stagecoach Road fault (SRF; Figure 6) was encountered at depths of about 100 m in two boreholes in the hanging wall. A whole-rock (minus mafics) K-Ar analysis of the pumice yielded an age of 8.5+/-3 Ma. Despite the large analytical uncertainty, the 8.5 Ma date is credible because this ash-fall unit is petrographically similar to several lavas and ash deposits with dates in the range of 8.5-to-7.5 Ma in the southwest part of the southwestern Nevada volcanic field, and no local units younger than 7.5 Ma resemble it. Based on the 100 m offset of this ash-fall deposit, the long-term slip rate across the Stagecoach Road fault has averaged about 0.012 mm/yr over the last 8.5 m.y. In contrast, offsets of late Pleistocene surficial deposits across this same fault in the same locality yield a late Quaternary slip rate of about 0.026 mm/yr.

Another example of slip-rate variation is seen in the trenches on the Solitario Canyon fault (SCF; Figure 6). Three to four coseismic surface ruptures occurred on this fault during the past 250,000 years that resulted in slightly more than 2 m of displacement (slip rate 0.008 mm/yr). In the same locality, a well-dated 900 ka soil is offset only 3 m, indicating a slip rate of only 0.0015 between 900 and 250 ka.

Data synthesized from all of the Quaternary faults in the Crater Flat basin define cyclic fluctuations in extensional faulting for the basin as a whole (Pezzopane, USGS, written comm., 1996). These data suggest that the rate of faulting has varied, typically over of an order of magnitude, over cycles of hundreds of thousands of years during the late Quaternary.

ACKNOWLEDGMENTS

This paper has benefited from the reviews from and discussions with numerous coworkers in the USGS, especially Dick Keefer, Ed DeWitt, Pete Rowley, and Dennis O'Leary. The figures were drafted by Michele Murray and Anne Tucker. Funding was supplied by the U. S. Department of Energy Yucca Mountain Project.

REFERENCES CITED

Ackerman, H. D., Mooney, W. D., Snyder, D. B., and Sutton, V. D., 1988, Preliminary interpretation of seismic-refraction and gravity studies west of Yucca Mountain, Nevada and California, *in*, Carr, M. D., and Yount, J. C., eds., Geologic and Hydrologic Investigations of a potential Nuclear Waste Disposal Site at Yucca Mountain, Nevada: U. S. Geological Survey Bulletin 1790, p. 23-33.

Bellier, O., and Zoback, M. L., 1995, Recent state of stress change in the Walker Lane zone, western Basin and Range province, United States: Tectonics, v. 14, p. 564-593.

Brocher, T. M., Hart, P. E., Hunter, W. C., and Langenheim, V. E., 1996, Hybrid-source seismic reflection profiling across Yucca Mountain, Nevada: regional lines 2 and 3: U. S. Geological Survey Open-File Report 96-28.

Carr, W. J., 1984, Regional structural setting of Yucca Mountain, southwestern Nevada, and late Cenozoic rates of tectonic activity in part of the southwestern Great Basin, Nevada and California: U. S. Geological Survey Open-File Report 84-854, 98 p.

Carr, W. J. and Parrish, L. D., 1985, Geology of drill hole USW VH-2, and structure of Crater Flat, southwestern Nevada: U. S. Geological Survey Open-File Report 85-475, 41 p.

Chapin, C. E. and Lowell, G. R., 1979, Primary and secondary flow structures in ash-flow tuffs of the Gribbles Run paleovalley, central Colorado: *in,* Smith, R. L., ed., Ash-flow Tuffs, Geological Society of America Special Paper 180, p. 137-154.

Christiansen, R. L., Lipman, P. W., Orkild, P. P., and Byers, F. M., Jr., 1965, Structure of the Timber Mountain caldera, southern Nevada and its relation to Basin-Range structure: U. S. Geological Survey Professional Paper 525-B, p. B43-48.

Connor, C. B., and Hill, B. E., 1995, Three nonhomogeneous Poisson models for the probability of basaltic volcanism: Application to the YM region, NV: Journal of Geophysical Research, v. 100, p. 10107-10125.

Crowe, B. M., Johnson, M. E., and Beckman, R. J., 1982, Calculation of the probability of volcanic disruption of a high-level repository within southern Nevada, USA: Radioactive Waste and the Nuclear Fuel Cycle, v. 3, p. 167-190.

Crowe, B. M., Perry, F. V., Geissman, J., McFadden, L. D., Wells, S. G., Murrell, M., Poths, J., Valentine, G. A., Bowker, L., and Finnegan, K., 1995, Status of volcanism studies for the Yucca Mountain site characterization project: Los Alamos National Laboratories report LA-12908-MS, Los Alamos, New Mexico, 363 p.

Cummings, D., 1968, Mechanical analysis of the effect of the Timber Mountain caldera on Basin and Range faults: Journal of Geophysical Research, v. 73, p. 2787-2794.

Faulds, J. E., Bell, J. W., Feuerbach, D. L., and Ramelli, A. R., 1994, Geologic map of the Crater Flat area, Nye County, Nevada: Nevada Bureau of Mines and Geology Map 101, 1:24,000 scale.

Ferrill, D. A., Stamatakos, J. A., Jones, S. M., Rahe, B., McKague, H. L., Martin, R. H., and Morris, A. P., 1996, Quaternary slip history of the Bare Mountain fault (Nevada) from the morphology and distribution of alluvial fan deposits: Geology, v. 24, p. 559-562.

Fisher, R. A., 1953, Dispersion on a sphere: Royal Society of London Proceedings, v. A217, p. 295-305.

Fox, K. F., Jr., and Carr, M. D., 1989, Neotectonics and volcanism at Yucca Mountain and vicinity, Nevada: Radioactive Waste Management and the Nuclear Fuel Cycle, v. 13, p. 37-50.

Fridrich, C. J., 1998, Tectonic evolution of the Crater Flat basin, Yucca Mountain region, Nevada: U. S. Geological Survey Open-File Report 98-XXX, 60 pp.

Fridrich, C. J., Crowe, B. M., Hudson, M. R., Langenheim, V. E., and Thompson, G. A., 1994, Structural control of basaltic volcanism in a region of oblique extension, southwest Nevada volcanic field: [abstr] EOS, Transactions of the American Geophysical Union, v. 75, p. 603.

Fridrich, C. J., Grauch, V. J. S., and Sawyer, D. A., 1996, Geophysical domains of the Nevada Test Site region and applications to regional hydrology [abstr]: Geological Society of America Abstracts with Programs, v. 28, no. 7, p. A192.

Geomatrix Consultants and TRW, 1996, Probabilistic Volcanic Hazards Analysis for Yucca Mountain, Nevada: Report BA0000000-01717-00082, prepared for the Department of Energy; available from TRW, 1261 Town Center Dr., Las Vegas, NV 89134.

Grauch, V. J. S., Sawyer, D. A., Hudson, M. R., Minor, S. A., and Cole, J. C., 1993, New detailed aeromagnetic data give fresh insight to mapping covered geologic units in the southwestern Nevada volcanic field: [abstr] American Geophysical Union (EOS), v. 74, p. 221.

Harmsen, S. C., 1994, The Little Skull Mountain earthquake of 29 June 1992: Aftershock focal mechanisms and tectonic stress field implications: Bulletin of the Seismological Society of America, v. 84, no. 5, p. 1484-1505.

Harmsen, S. C., and Bufe, C. G., 1992, Seismicity and focal mechanisms in the southern Great Basin of Nevada and California: 1987 through 1989: U. S. Geological Survey Open-File Report 91-572, 216 p.

Hoisch, T. D., Heizler, M. T., and Zartman, R. E., 1997, Timing of detachment faulting in the Bullfrog Hills and Bare Mountain area, southwest Nevada: Inferences from $^{40}Ar/^{39}Ar$, K-Ar, U-Pb, and fission-track thermochronology: Journal of Geophysical Research, v. 102, p. 2815-2833.

Hudson, M. R., Minor, S. A., and Fridrich, C. J., 1996, The distribution, timing, and character of steep-axis rotations in a broad zone of dextral shear in southwestern Nevada [abstr]: Geological Society of America Abstracts with Programs, v. 28, no. 7, p. A451.

Hudson, M. R., Sawyer, D. A., and Warren, R. G., 1994, Paleomagnetism and rotation constraints for the middle Miocene southwestern Nevada volcanic field: Tectonics, v. 13, p. 258-277.

Kirschvink, J. L., 1980, Least-squares line and plane and analysis of paleomagnetic data: Gerophysical Journal of the Royal Astronomical Society, v. 62, p. 699-718.

Klinger, R. E. and Anderson, L. W., 1993, Preliminary evaluation of the Bare Mountain fault zone, Nye County, Nevada: Seismotectonic Report 93-6, U. S. Bureau of Reclamation, Denver, Colorado, 15 p.

Menges, C. M., Wesling, J. R., Whitney, J. A., Swan, F. H., Coe, J. A., Thomas, A. P., and Oswald, J. A., 1994, Preliminary results of paleoseismic investigations of Quaternary faults on eastern Yucca Mountain, Nye County, Nevada: High-Level Radioactive Waste Management, Proceedings of the Fifth Annual International Conference, American Nuclear

Society, Las Vegas, Nevada, v. 4, p. 2373-2390.

Minor, S. A., Hudson, M. R., and Fridrich, C. J., 1996, Fault-slip data bearing on the tectonic development of northern Crater Flat basin, southern Nevada [abstr]: Geological Society of America Abstracts with Programs, v. 28, no. 7, p. A192.

Nur, A., Ron, H., and Scotti, O., 1986, Fault mechanics and the kinematics of block rotations: Geology, v. 14, p. 746-749.

_____, 1989, Mechanics of distributed fault and block rotation, *in*, C. Kissel and C. Laj, eds., Paleomagnetic Rotations and Continental Deformation, Kluwer Academic Publishers, p. 209-228.

Parsons, T., and Thompson, G. A., 1991, The role of magma overpressure in suppressing earthquakes and topography: World-wide examples: Science, v. 253, p. 1399-1402.

Pezzopane, S. K., Menges, C. M., and Whitney, J. W., 1994, Quaternary paleoseismology and Neogene tectonics at Yucca Mountain, Nevada: Proceedings of the Workshop on Paleoseismology, Marshall, California, National Earthquake Hazards Reduction Program: U. S. Geological Survey Open-File Report 94-568, p. 149-151.

Rosenbaum, J. G., Hudson, M. R., and Scott, R. B., 1991, Paleomagnetic constraints on the geometry and timing of deformation at Yucca Mountain, Nevada: Journal of Geophysical Research, v. 96, p. 1963-1980.

Sawyer, D. A., Fleck, R. J., Lanphere, M. A., Warren, R. G., Broxton, D. E., and Hudson, M. R., 1994, Episodic caldera volcanism in the Miocene southwest Nevada volcanic field: Revised stratigraphic framework, $^{40}Ar/^{39}Ar$ geochronologic framework, and implications for magmatism and extension: Geological Society of America Bulletin, v. 106, no. 10, p. 1304-1318.

Scott, R. B., 1990, Tectonic setting of Yucca Mountain, southwest Nevada, *in*, Wernicke, B. P., ed., Basin and range extensional tectonics near the latitude of Las Vegas, Nevada: Geological Society of America Memoir 176, p. 251-282.

Scott, R. B., and Bonk, J., 1984, Preliminary geologic map of Yucca Mountain with geologic sections, Nye County, Nevada: U. S. Geological Survey Open-File Report 84-494, 1:12,000 scale.

Simonds, F. W., Whitney, J. W., Fox, K. F., Ramelli, A. R., Yount, J. C., Carr, M. D., Menges, C. M., Dickerson, R. P., and Scott, R. B., 1995, Map showing fault activity in the Yucca Mountain area, Nye County, Nevada: U. S. Geological Survey map I-2520, scale 1:24,000.

Smith, E. I., Feuerbach, D. L., Naumann, T. R., and Faulds, J. E., 1991, The area of most recent volcanism near Yucca Mountain, Nebada: 0Imoplicatiomns fot volc risk assessmenrt: in High-level Radioactive waste management, Prodceedinbgs of the 3rd annual international conferenvce, LV, NV April 8-12, 1990, American Nuclear Society, La Grange Park Illinois, 1990, p. 81-90.

Snyder, D. B., and Carr, W. J., 1984, Interpretation of gravity in a complex volcano-tectonic setting, southwestern Nevada: Journal of Geophysical Research, v. 89, no. B12, p. 10,193-10,206.

Stewart, J. H., 1988, Tectonics of the Walker Lane belt, western Great Basin-Mesozoic and Tertiary deformation in a zone of shear, *in*, Ernst, W. G., ed., Metamorphism and crustal evolution of the western United States, Rubey Vol. VII: Englewood Cliffs, New Jersey, Prentice Hall, p. 683-713.

Swadley, W C, and Carr, W. J., 1987, Geologic map of the Quaternary and Tertiary deposits of the Big Dune Quadrangle, Nye County, Nevada and Inyo County, California: U. S. Geological Survey Map I-1767: scale 1:48,000.

FIGURE CAPTIONS

Figure 1: Structural domains and domain boundaries of the Yucca Mountain region and internal structures of the Crater Flat basin and selected parts of adjacent domains, and distribution of basalts of different ages in relation to basin structure.

Figure 2: (A) Tilt domain map showing average dips of the 12.7 Ma Tiva canyon Tuff, corrected for post-11.6-Ma tilting of the Rainier Mesa Tuff. (B) Map showing areas with differing percentages of extension within Crater Flat basin from 12.7 to 11.6 Ma; maximum (top) and minimum (bottom, in parens) estimates based on the corrected tilts and using the equation of Nur and others (1989).

Figure 3: (A) Tilt domain map showing average dips of the 11.6 Ma Rainier Mesa Tuff, corrected for post-10.5-Ma tilting. (B) Map showing areas with differing percentages of extension within Crater Flat basin from 11.6 to 10.5 Ma; maximum (top) and minimum (bottom, in parens) estimates based on the corrected tilts and using the equation of Nur and others (1989).

Figure 4: (A) Tilt domain map showing average dips of the 10.5 Ma basalts and breccias. (B) Map showing areas with differing percentages of extension within Crater Flat basin from 10.5 Ma to present; maximum (top) and minimum (bottom, in parens) estimates based on the tilts and using the equation of Nur and others (1989).

Figure 5: Contour maps showing areal variation of the estimated cumulatrive percent of extension (of the 12.7 Ma Tiva Canyon Tuff) from the initiation of the Crater Flat basin to the present: (A) Maximum estimates; (B) Minimum estimates.

Figure 6: Map showing identified Quaternary faults of the Crater Flat basin and slip rates in mm/yr determined from trenching studies; slip rates in parens are inferred. Dashed

lines are transects normal to extension.

Figure 7: (A) Graph of estimated extension rates in Crater Flat basin from the middle Miocene to the present. (B) Graph of magma erupted over time in the Crater Flat basin.

Figure 8: Map showing areal variations of measured vertical-axis rotations of selected volcanic units within the Crater Flat basin, with contours showing total rotation from the initiation of Crater Flat basin, at 12.7 Ma, to the present.

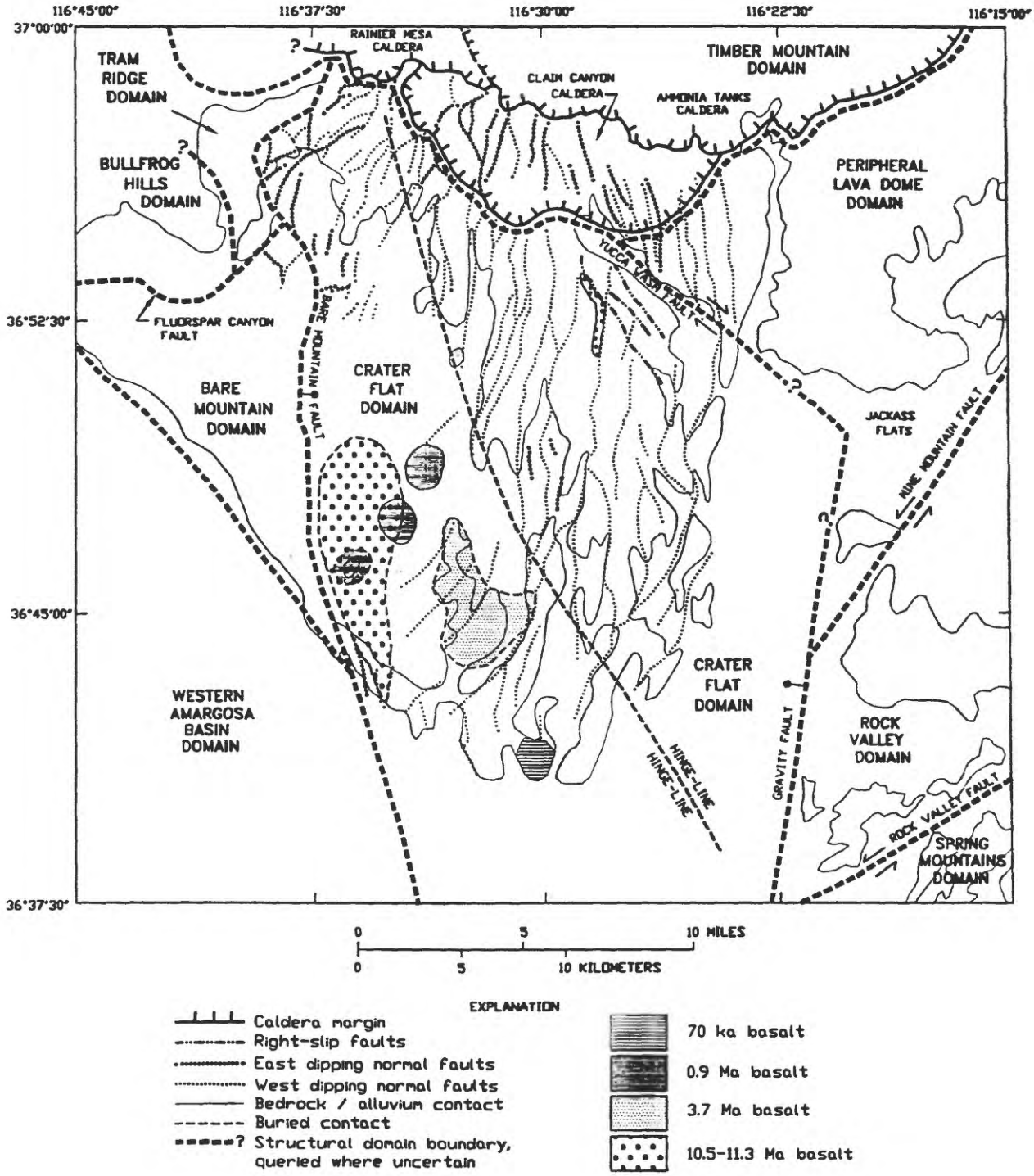
116°45'00"
116°37'30"
116°30'00"
116°22'30"
116°15'00"
37°00'00"
36°52'30"
36°45'00"
36°37'30"
RAINIER MESA CALDERA
CLAIM CANYON CALDERA
AMMONIA TANKS CALDERA
TIMBER MOUNTAIN DOMAIN
TRAM RIDGE DOMAIN
BULLFROG HILLS DOMAIN
PERIPHERAL LAVA DOME DOMAIN
YUCCA MTN. FAULT
FLUORSPAR CANYON FAULT
BARE MOUNTAIN FAULT
BARE MOUNTAIN DOMAIN
CRATER FLAT DOMAIN
JACKASS FLATS
NINE MOUNTAIN FAULT
WESTERN AMARGOSA BASIN DOMAIN
HINGE-LINE
GRAVITY FAULT
ROCK VALLEY DOMAIN
ROCK VALLEY FAULT
SPRING MOUNTAINS DOMAIN
0 5 10 MILES
0 5 10 KILOMETERS
EXPLANATION
Caldera margin
Right-slip faults
East dipping normal faults
West dipping normal faults
Bedrock / alluvium contact
Buried contact
Structural domain boundary, queried where uncertain
70 ka basalt
0.9 Ma basalt
3.7 Ma basalt
10.5-11.3 Ma basalt

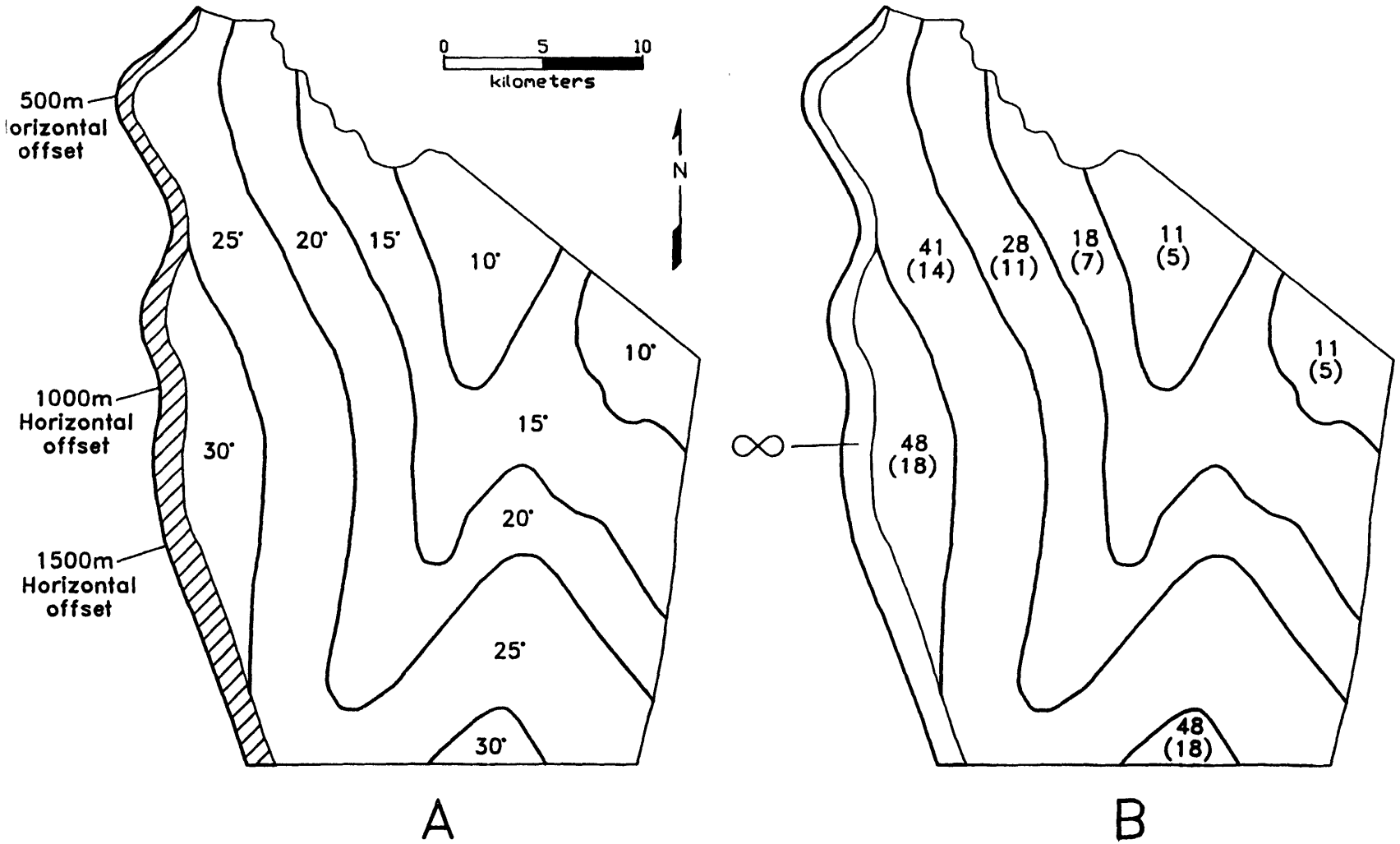
0 5 10
kilometers
N
500m
Horizontal
offset
1000m
Horizontal
offset
1500m
Horizontal
offset
25°
20°
15°
10°
10°
15°
30°
20°
25°
30°
∞
41
(14)
28
(11)
18
(7)
11
(5)
11
(5)
48
(18)
48
(18)
A
B

FIGURE 2

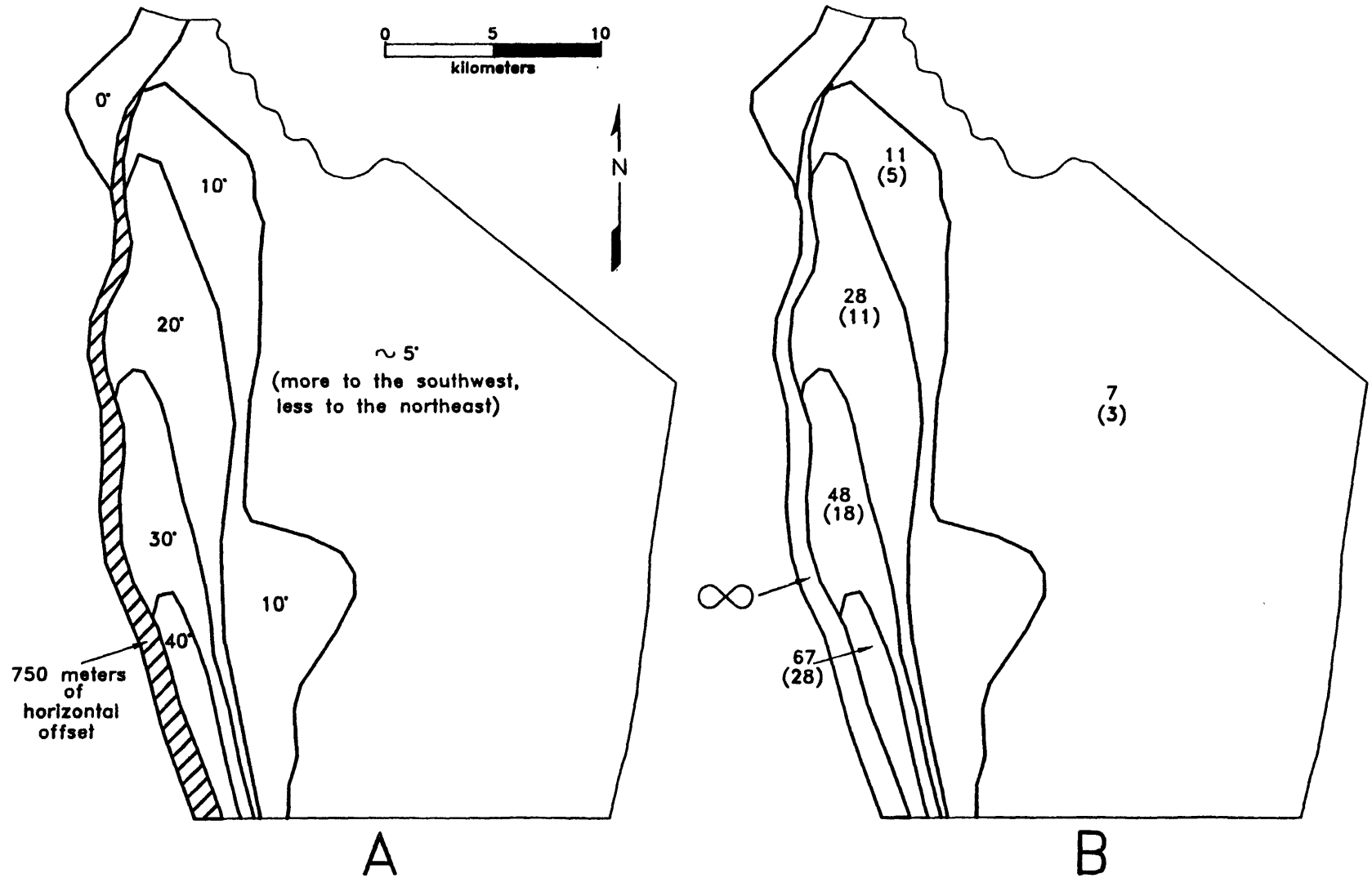
0
5
10
kilometers
N
0°
10°
20°
30°
40°
10°
~ 5°
(more to the southwest,
less to the northeast)
750 meters
of
horizontal
offset
A
11
(5)
28
(11)
7
(3)
48
(18)
∞
67
(28)
B

FIGURE 3

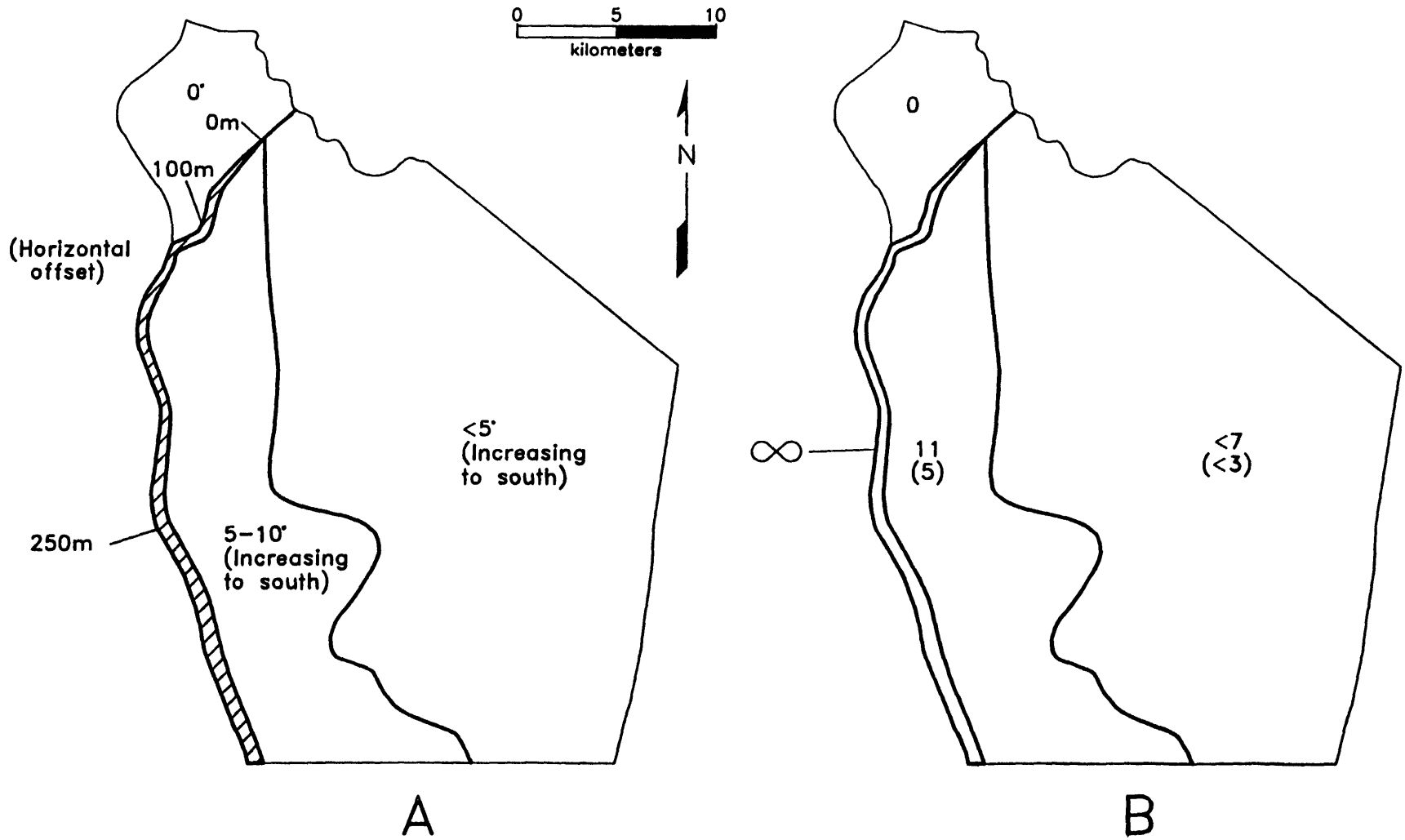
0
5
10
kilometers
N
0°
0m
100m
(Horizontal offset)
250m
5–10°
(Increasing to south)
<5°
(Increasing to south)
A
0
∞
11
(5)
<7
(<3)
B

FIGURE 4

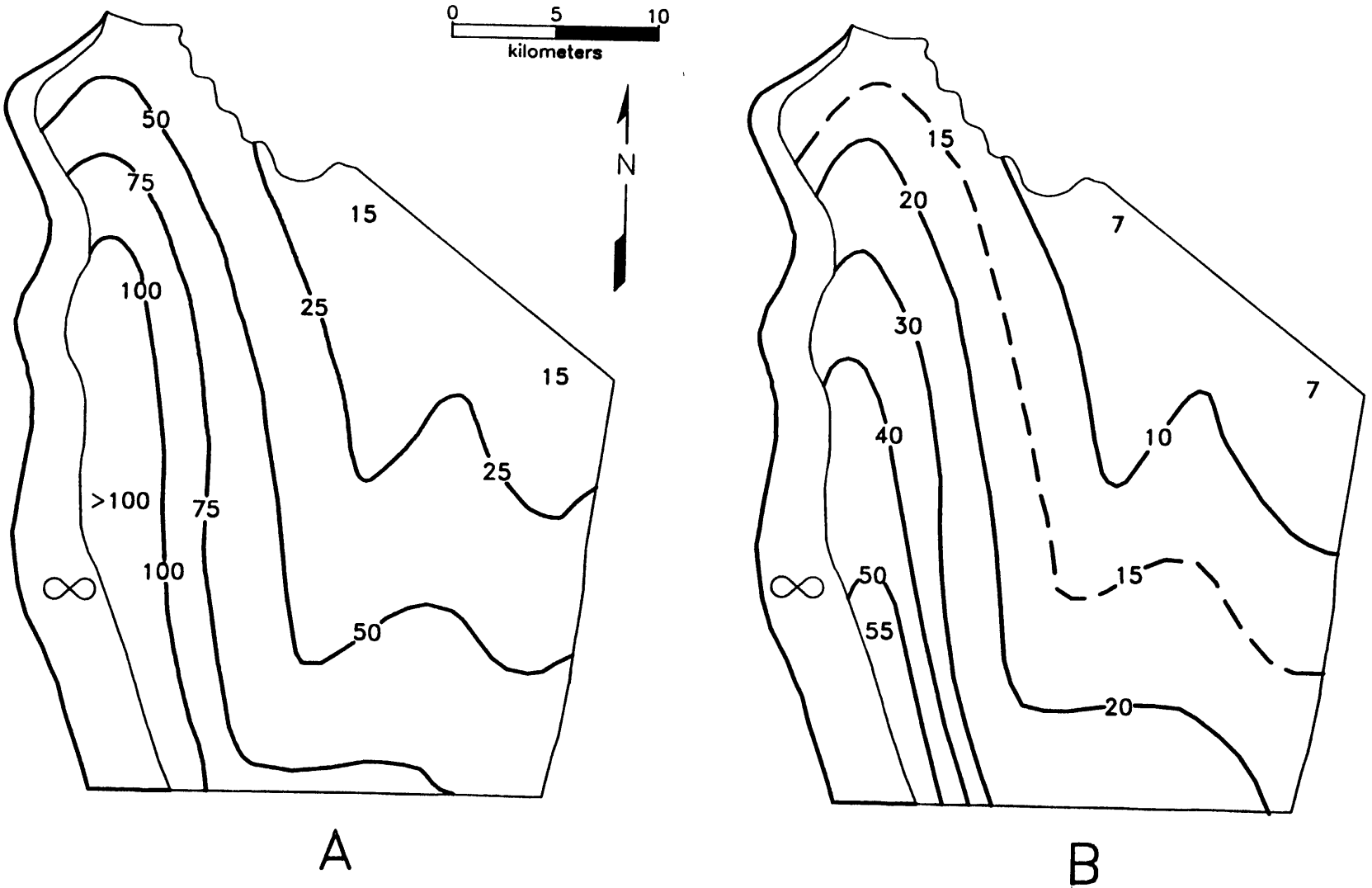
0
5
10
kilometers
N
50
75
100
>100
75
100
∞
15
25
15
25
50
A
15
20
30
40
∞
50
55
7
7
10
15
20
B

FIGURE 5

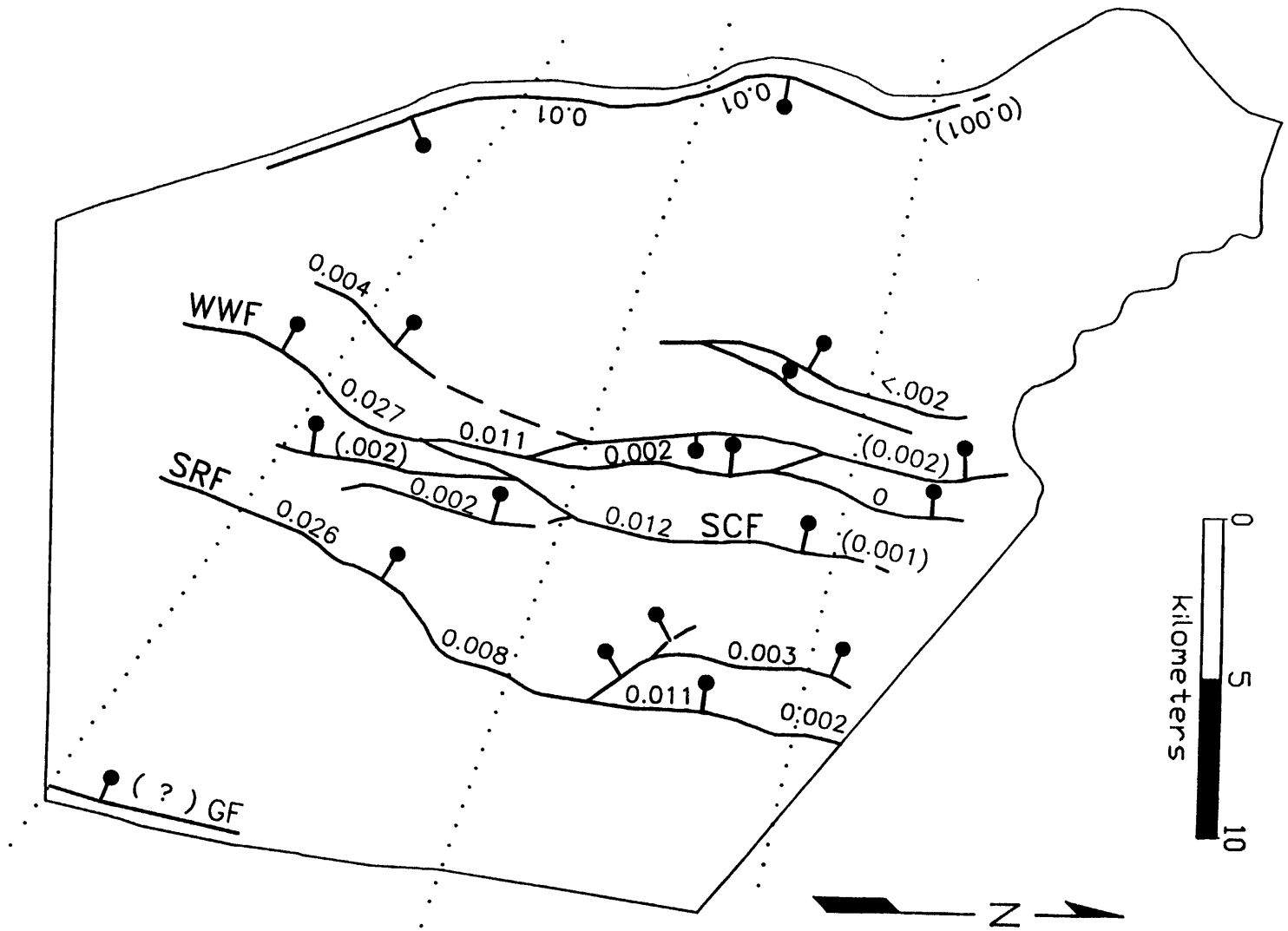
0.01
0.01
(0.001)
0.004
WWF
0.027
0.011
0.002
<.002
(.002)
(0.002)
SRF
0.002
0
0.026
0.012
SCF
(0.001)
0.008
0.003
0.011
0.002
(?) GF
0
5
10
kilometers
N

FIGURE 6

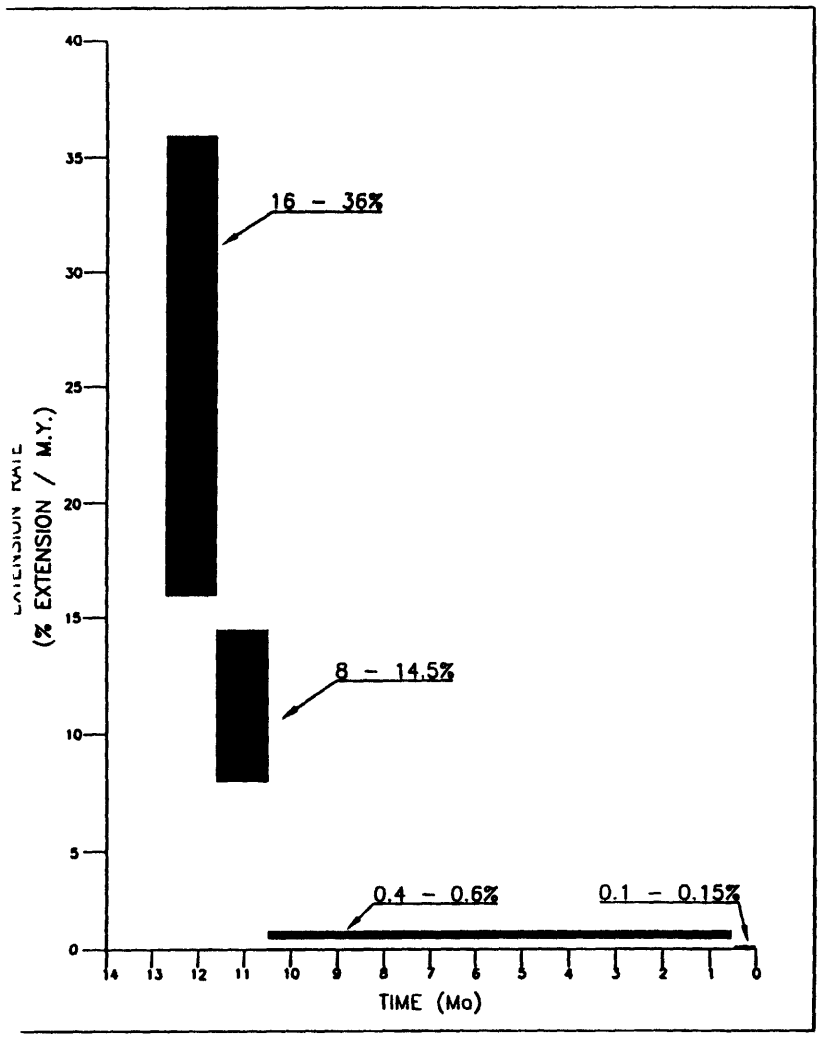
(% EXTENSION / M.Y.)
40
35
30
25
20
15
10
5
0
16 - 36%
8 - 14.5%
0.4 - 0.6%
0.1 - 0.15%
14 13 12 11 10 9 8 7 6 5 4 3 2 1 0
TIME (Ma)

A

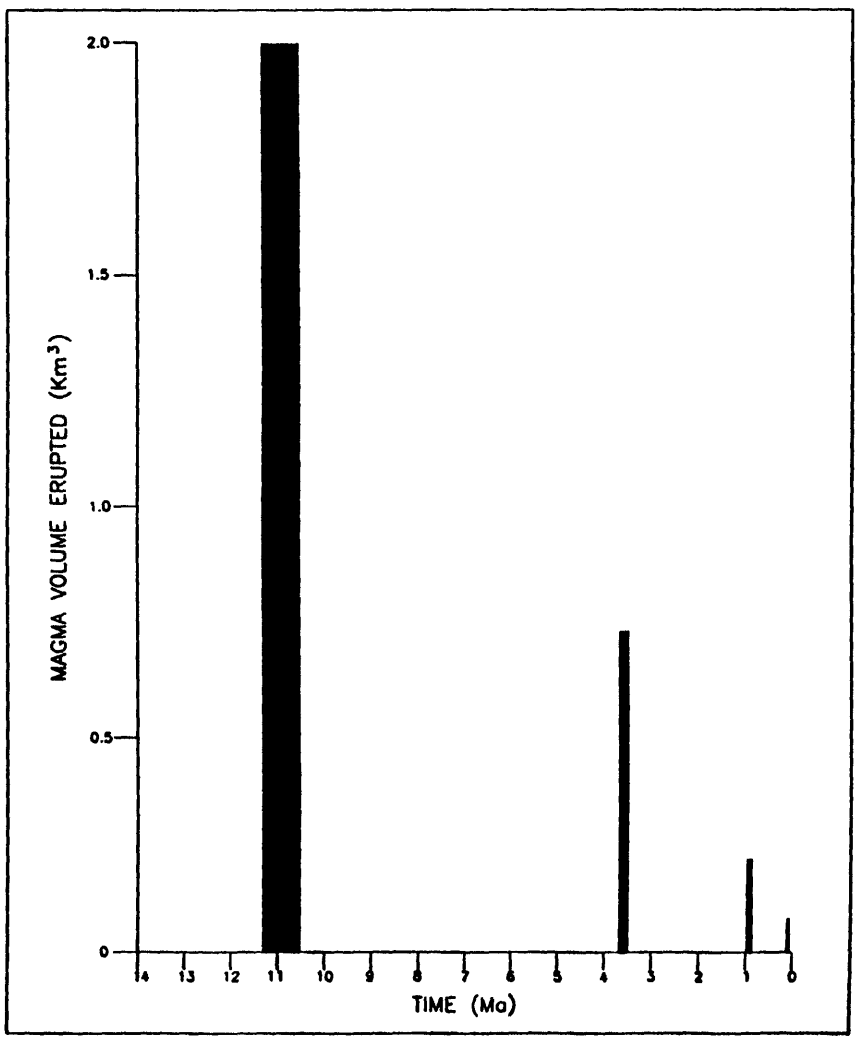
MAGMA VOLUME ERUPTED (Km³)
2.0
1.5
1.0
0.5
0
14 13 12 11 10 9 8 7 6 5 4 3 2 1 0
TIME (Ma)

B

FIGURE 7

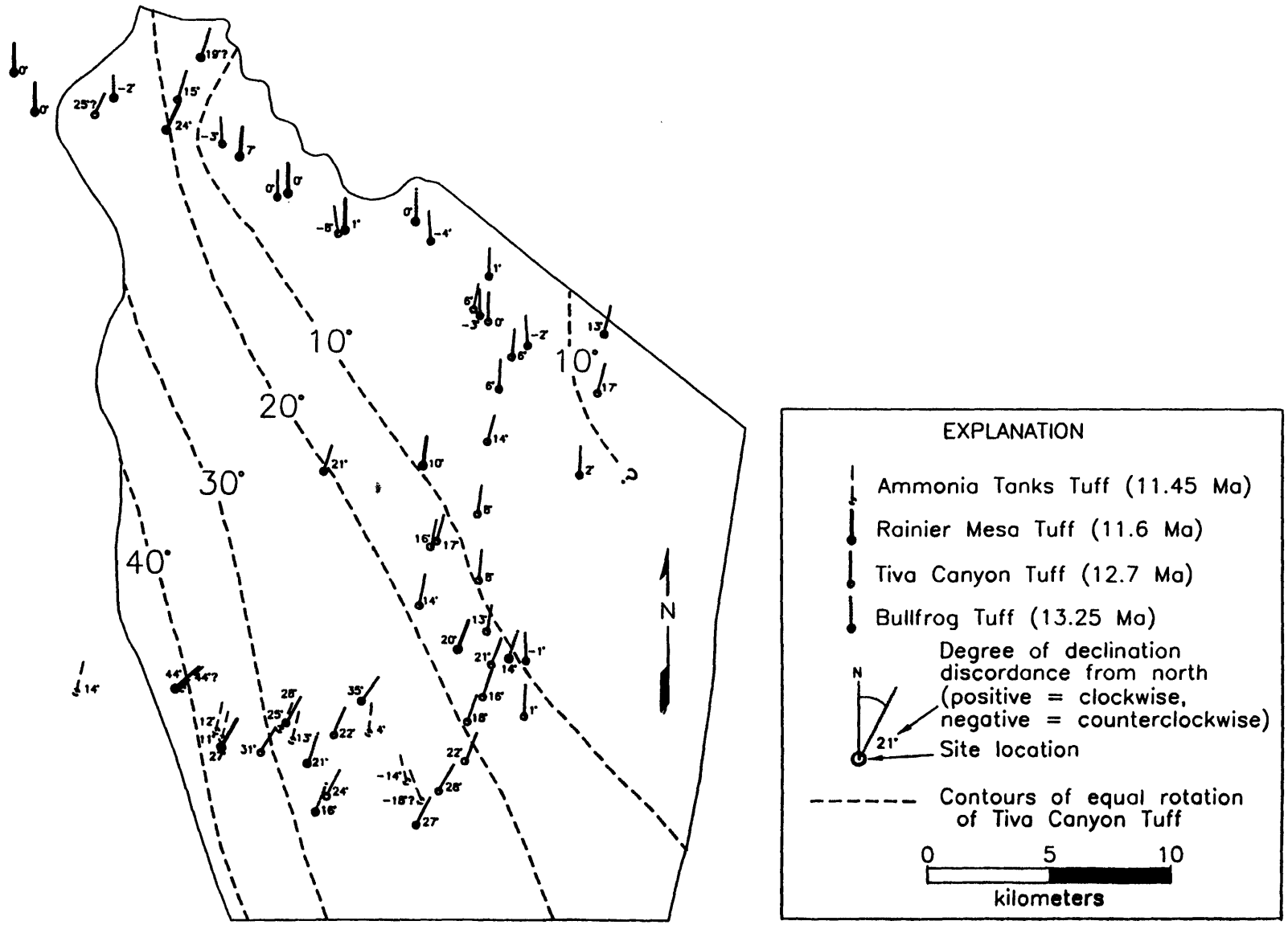
10°
20°
30°
40°
N
EXPLANATION
Ammonia Tanks Tuff (11.45 Ma)
Rainier Mesa Tuff (11.6 Ma)
Tiva Canyon Tuff (12.7 Ma)
Bullfrog Tuff (13.25 Ma)
Degree of declination discordance from north (positive = clockwise, negative = counterclockwise)
Site location
Contours of equal rotation of Tiva Canyon Tuff
0
5
10
kilometers

FIGURE 8